

Competitive Inhibition at the Glycine Site of the *N*-Methyl-D-Aspartate Receptor Mediates Xenon Neuroprotection against Hypoxia–Ischemia

Paul Banks, B.Sc.,* Nicholas P. Franks, Ph.D., F.R.C.A., F.Med.Sci.,† Robert Dickinson, Ph.D.‡

ABSTRACT

Background: The general anesthetic gas xenon is neuroprotective and is undergoing clinical trials as a treatment for ischemic brain injury. A small number of molecular targets for xenon have been identified, the *N*-methyl-D-aspartate (NMDA) receptor, the two-pore-domain potassium channel TREK-1, and the adenosine triphosphate-sensitive potassium channel (K_{ATP}). However, which of these targets are relevant to acute xenon neuroprotection is not known. Xenon inhibits NMDA receptors by competing with glycine at the glycine-binding site. We test the hypothesis that inhibition of the NMDA receptor at the glycine site underlies xenon neuroprotection against hypoxia–ischemia.

Methods: We use an *in vitro* model of hypoxia–ischemia to investigate the mechanism of xenon neuroprotection. Organotypic hippocampal brain slices from mice are subjected to oxygen–glucose deprivation, and injury is quantified by propidium iodide fluorescence.

Results: We show that 50% atm xenon is neuroprotective against hypoxia–ischemia when applied immediately after injury or after a delay of 3 h after injury. To validate our method, we show that neuroprotection by gvestinel is abolished when glycine is added, confirming that NMDA receptor glycine site antagonism underlies gvestinel neuroprotection. We then show that adding glycine abolishes the neuroprotective effect of xenon, consistent with competitive inhibition at the NMDA receptor glycine site mediating xenon neuroprotection.

Conclusions: We show that xenon neuroprotection against hypoxia–ischemia can be reversed by increasing the glycine concentration. This is consistent with competitive inhibition by xenon at the NMDA receptor glycine site, playing a significant role in xenon neuroprotec-

tion. This finding may have important implications for xenon's clinical use as an anesthetic and neuroprotectant.

What We Already Know about This Topic

- ❖ The anesthetic gas xenon is neuroprotective and also blocks *N*-methyl-D-aspartate (NMDA) receptors, but whether these effects are related is not known

What This Article Tells Us That Is New

- ❖ In mouse, hippocampus cultures xenon protected injury from hypoxia, and this effect was inhibited by increasing concentrations of glycine
- ❖ Xenon may be neuroprotective by blocking NMDA receptors via binding to its glycine site

ISCHEMIC brain injury is a major financial burden for healthcare providers across the globe. In the United States, stroke is the third most common cause of death, accounting for 1 in 16 of all deaths in 2004,¹ and it is the leading cause of severe disability. Currently, there are no treatments specifically targeted at limiting neuronal death after ischemia. The inert gas xenon has neuroprotective properties^{2–5} and is a particularly attractive candidate as a neuroprotectant because it rapidly crosses the blood–brain barrier, exhibits cardiovascular stability, and cannot be metabolized.^{6,7} The fact that xenon can cause general anesthesia has been known since the 1950s,⁸ but its mechanism of action remained a mystery. In our search for the molecular targets underlying xenon anesthesia, we discovered that xenon is an *N*-methyl-D-aspartate (NMDA) receptor antagonist,⁹ which prompted investigation of its use as a neuroprotectant. Xenon has now been evaluated as a neuroprotectant in a variety of different settings,^{2–5} and it is about to begin clinical trials for use in neonatal asphyxia, but the mechanisms by which xenon causes neuroprotection have not been clearly identified. The action of xenon as an NMDA receptor antagonist provides a plausible explanation of its neuroprotective properties. However, whether NMDA receptor antagonism actually underlies xenon neuroprotection has not been determined. We recently made an advance in our understanding of the action of xenon at NMDA receptors by showing that it competes with the coagonist glycine.¹⁰ This

* Ph.D. Student, † Professor of Biophysics and Anaesthetics, ‡ Lecturer in Anaesthetics, Biophysics Section, Blackett Laboratory, and Department of Anaesthetics, Pain Medicine and Intensive Care, Imperial College London.

Received from Blackett Laboratory, Imperial College London, South Kensington, London, United Kingdom. Submitted for publication July 2, 2009. Accepted for publication November 19, 2009. Supported by the European Society for Anaesthesiology, Brussels, Belgium; The Royal College of Anaesthetists, London, United Kingdom; Westminster Medical School Research Trust, London, United Kingdom (to Dr. Banks); and Air Products and Chemicals, Inc., Allentown, Pennsylvania. Prof. Franks has a financial interest in the use of xenon as a neuroprotectant and is a paid consultant for Air Products and Chemicals Inc. for this activity.

Address correspondence to Dr. Dickinson: Blackett Laboratory, Imperial College London, South Kensington, London SW7 2AZ, United Kingdom. r.dickinson@imperial.ac.uk. Information on purchasing reprints may be found at www.anesthesiology.org or on the masthead page at the beginning of this issue. ANESTHESIOLOGY's articles are made freely accessible to all readers, for personal use only, 6 months from the cover date of the issue.

new finding provides a pharmacologic method of testing whether NMDA receptor inhibition mediates xenon neuroprotection. We showed that xenon inhibits NMDA receptors less at higher glycine concentrations.¹⁰ If NMDA receptor glycine site antagonism mediates xenon neuroprotection, the degree of neuroprotection should also be less at higher glycine concentrations.¹¹ In this study, we test the hypothesis that xenon neuroprotection against hypoxia–ischemia is mediated by inhibition of the NMDA receptor glycine-binding site. We use an *in vitro* model of hypoxia–ischemia using organotypic hippocampal brain-slice cultures from mice subjected to oxygen-glucose deprivation (OGD) and with injury quantified by propidium iodide (PI) fluorescence.

Materials and Methods

Hippocampal Organotypic Slices

All experiments were performed in compliance with the Ethical Review Committee of Imperial College (London, United Kingdom) and the United Kingdom Animals (Scientific Procedures) Act of 1986. All efforts were made to minimize animal suffering and the number of animals used. Unless otherwise stated, chemicals were obtained from Sigma Chemical Company Ltd (Poole, Dorset, United Kingdom). Organotypic hippocampal slice cultures were prepared as previously described¹² with some modifications. In brief, brains were removed from 7-day-old C57/BL6 mouse pups (Harlan Ltd., Bicester, Oxfordshire, United Kingdom) and placed in ice-cold “preparation” medium. The preparation medium contained Gey’s balanced salt solution, 5 mg/ml D-glucose (Fisher Scientific, Loughborough, Leicestershire, United Kingdom) and 1% antibiotic-antimycotic suspension. The hippocampi were removed from the brains, and 400- μ M thick transverse slices were prepared using a McIlwain tissue chopper. Slices were transferred into ice-cold preparation medium, gently separated, and then placed onto tissue culture inserts (Millicell-CM; Millipore Corporation, Carrigtwohill, Co. Cork, Ireland), which were inserted into a six-well tissue culture plate. The wells contained “growth” medium consisting of 50% Minimal Essential Media Eagle, 25% Hank’s balanced salt solution, 25% inactivated horse serum, 2 mM L-glutamine, 5 mg/ml D-glucose, and 1% antibiotic-antimycotic suspension. Slices were incubated at 37°C in a 95% air/5% CO₂ humidified atmosphere. The growth medium was changed every 3 days. Experiments were performed after 14 days in culture.

OGD and Hyperbaric Gas Chamber

After the hippocampal slices had been in culture for 14 days, the growth medium was changed to “experimental” medium. The experimental medium was serum free and consisted of 75% Minimal Essential Media Eagle, 25% Hank’s balanced salt solution, 2 mM L-glutamine, 5 mg/ml D-glucose, 1% antibiotic-antimycotic suspension, and 4.5 μ M PI. Thirty minutes after transfer to experimental media, the slices were imaged to assess slice viability before OGD. Typ-

ically, slices exhibited little PI fluorescence, an indicator of healthy slices. A small number of slices showed regions of dense staining, indicating compromised viability, presumably because of mechanical damage during the slice preparation stage. These slices were excluded from further analysis. Immediately after initial imaging, experimental medium was exchanged for “OGD medium,” 120 mM NaCl, 5 mM KCl, 1.25 mM NaH₂PO₄, 2 mM MgSO₄, 2 mM CaCl₂, 25 mM NaHCO₃, 10 mM sucrose, and 20 mM HEPES, pH 7.25 or “sham medium,” which had the same composition, except that sucrose was replaced with 10 mM D-glucose. OGD medium was deoxygenated before use by bubbling for 45 min at 50 ml/min with 95% N₂/5% CO₂, in a Dreschel bottle, using a fine-sintered glass bubbler and filter sterilized using a 0.2- μ M filter. Sham media was treated in the same way, except that it was bubbled with 20% O₂/75% N₂/5% CO₂. After solution exchange, the culture trays were transferred to a small pressure chamber (see fig. 1A) containing a high-speed fan for rapid gas mixing. The pressure chamber was housed in an incubator set at 37°C. The chamber (gas volume 0.925 l) was flushed with humidified gas (95% N₂/5% CO₂ or 20% O₂/75% N₂/5% CO₂) for 5 min at 5 l/min, which would ensure better than 99.99% gas replacement. After flushing, the pressure chamber was sealed for a set period (2, 5, 10, 20, 30, 60, or 90 min), which constituted the duration of OGD (or sham treatment).

After the period of OGD, slices were removed from the chamber and medium was replaced with experimental medium (in experiments with gavestinel or added glycine, this was added for the first time at this stage). A schematic of a typical experiment is shown in figure 1B. Because of its limited aqueous solubility, gavestinel was added to the media from a concentrated stock in dimethyl sulfoxide, the final dimethyl sulfoxide concentration was 0.01% vol/vol. The same amount of dimethyl sulfoxide was added to the sham-treated and OGD slices for the gavestinel experiments. The addition of dimethyl sulfoxide had no significant effect on sham-treated ($P = 0.32$) or OGD slices ($P = 0.42$). Slices were returned to the chamber, which was flushed with 20% O₂/75% N₂/5% CO₂ as before and sealed. In xenon experiments, 0.5 atm of xenon was added after sealing the chamber, in addition to the 1 atm of 20% O₂/75% N₂/5% CO₂, with helium used in place of xenon in control experiments. The chamber fan was left on for 5 min to achieve mixing of xenon or helium. After 24 h in the chamber, the slices were imaged using a fluorescent microscope (see Quantifying Cell Injury section). In some experiments, this procedure was repeated at other time points after OGD. Note that, for all gas mixtures (except during OGD), the partial pressures of oxygen and carbon dioxide were fixed at 0.2 and 0.05 atm, respectively. During OGD, the partial pressures were 0.95 atm nitrogen and 0.05 atm carbon dioxide.

Quantifying Cell Injury

PI is a membrane-impermeable dye that enters only the cells with damaged cell membranes.¹³ Inside the cells it binds

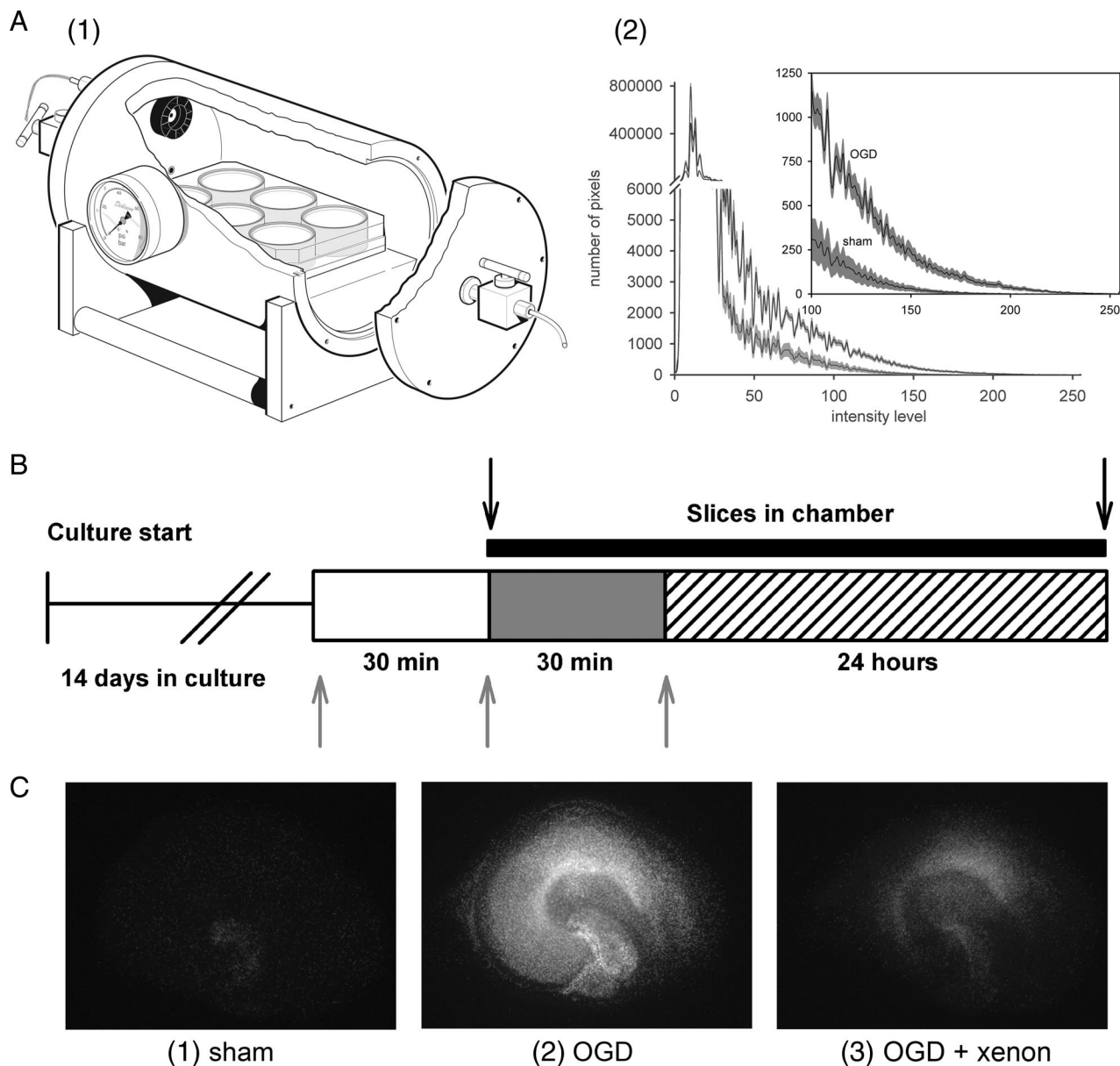


Fig. 1. (A, 1) Experimental chamber for exposure of slices to oxygen-glucose deprivation (OGD) and xenon. Organotypic hippocampal brain-slice cultures grown on membrane inserts in six-well cell culture plates are placed inside the chamber. The chamber is equipped with a small fan (shown in *black*) for mixing of humidified gases. The whole chamber is placed inside an incubator at 37°C. (2) Intensity histograms (*black line*) showing distribution of fluorescence intensity for hippocampal slices 24 h after OGD ($n = 68$ slices) or sham treatment ($n = 26$ slices). The shaded envelope around each line indicates the SEM. Injury was quantified by integrating the area under the curves above an intensity level of 100. Inset shows an expanded view of intensity level above this threshold. (B) Schematic representation of a typical OGD experiment. (*black arrows*) Fluorescence imaging of slices, (*gray arrows*) changes of culture medium, and colored areas represent different culture media: (*white*) experimental medium, (*dark gray*) OGD medium, and (*hatched*) experimental medium with added glycine, gavestinel, and xenon where appropriate, (*black bar*) period where slices are housed in the chamber. (C) Typical propidium iodide (PI) fluorescence images of organotypic slices subjected to (1) sham-treatment, (2) oxygen-glucose deprivation, or (3) OGD plus xenon. PI is a membrane impermeable dye that enters only cells with damaged cell membranes where it becomes highly fluorescent on binding to DNA.

principally to DNA and becomes highly fluorescent, with a peak emission spectrum in the red region of the visible spectrum. An epi-illumination microscope (Nikon Eclipse 80, Kingston upon Thames, Surrey, United Kingdom) and a low-power (2×) objective were used to visualize the PI fluo-

rescence. A digital video camera and software (Micropublisher 3.3 RTV camera and QCapture Pro software; Qimaging, Inc., Surrey, British Columbia, Canada) were used to capture the images. The images were analyzed using ImageJ software. Red, green, and blue channels were recorded, but only the red channel was used, and the distribution of intensities was plotted as a histogram with 256 intensity levels.

§ <http://rsb.info.nih.gov>. Accessed November 6, 2009.

Slices under standard control (sham) conditions, incubated in the chamber for 24 h at 37°C with 20% O₂/75% N₂/5% CO₂, showed little PI fluorescence compared with OGD-treated slices that showed bright PI fluorescence (fig. 1C). To quantify the injury, we integrated the number of pixels above a threshold of 100 (see inset fig. 1A), which provided a robust quantitative measurement of PI fluorescence and hence of cell injury. In the experiments on the evolution of injury after OGD (see fig. 2), to increase the sensitivity of the measurement, a threshold of 50 was used. Because the light output from the mercury lamp changed over time, the exposure time was adjusted to take this into account. This was performed by recording fluorescence from a glass slide standard (Fluor-Ref, Omega Optical, Brattleboro, VT) and adjusting the exposure time accordingly.

Statistics

The error bars are shown as SEM. Our sample sizes (30–60 slices) were sufficiently large for the central limit theorem to be applicable. Unless stated otherwise, we assessed significance using a two-tailed unpaired Student *t* test. We compared control OGD under multiple conditions, using ANOVA with Tukey *post hoc* test. *P* values of less than 0.05 were considered to indicate a significant difference between groups. Statistical tests were implemented using the SigmaPlot (Systat Inc., Point Richmond, CA) or SPSS (SPSS Inc., Chicago, IL) software packages.

Results

Slices subjected to OGD exhibited a bright PI fluorescence compared with sham-treated slices (fig. 1C). To determine the optimum time of OGD for our standard control injury, we investigated the degree of cell injury, quantified by PI fluorescence, as a function of duration of OGD. Periods of OGD \geq 2-min duration resulted in cell injury, with injury appearing to plateau at around 30–60 min of OGD, as shown in figure 2A. We chose 30 min of OGD as our standard insult because this gave a robust and reproducible increase in fluorescence. Then, we characterized the development of the injury as a function of time after OGD. As shown in figure 2B, injury became apparent 3 h after OGD and developed fully between 6 and 24 h. There was no increase in injury between 24 and 72 h after OGD. We therefore chose 24 h as the standard point at which to quantify injury. Because 30-min OGD gave a robust fluorescence that appeared close to maximal, we chose to normalize our data to this point. Sham-treated slices underwent identical solution exchanges as the OGD slices (see fig. 1B), except that solutions contained normal oxygen and glucose concentrations. Because the xenon neuroprotection experiments would use 0.5 atm pressure of xenon, we determined whether pressure *per se* would affect the slices. We determined the effect of 0.5 atm pressure of helium on both sham-treated and OGD-treated slices. Helium was chosen because it is unlikely to exert any pharmacologic effect of its own at these low pres-

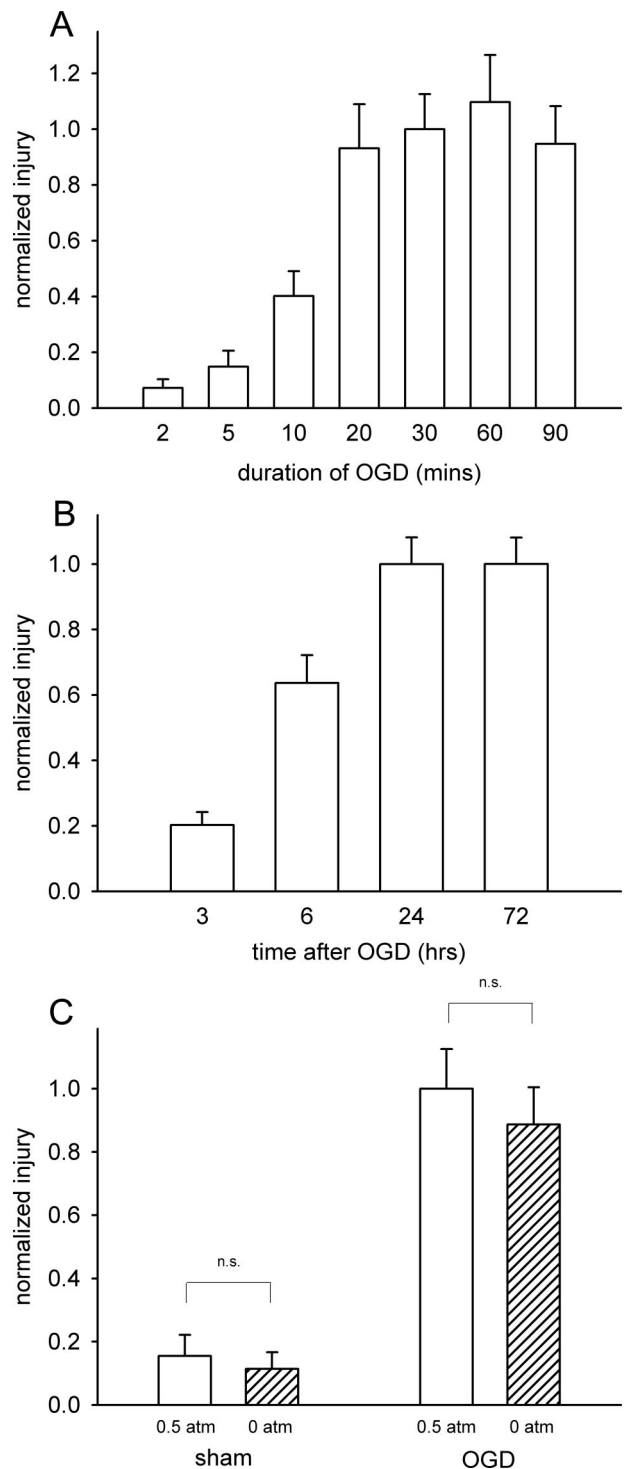


Fig. 2. (A) Extent of injury, quantified by propidium iodide fluorescence intensity, as a function of time of oxygen-glucose deprivation (OGD). Organotypic hippocampal slices are sensitive to periods of OGD from 2- to 90-min duration. The fluorescence intensity was measured 24 h after OGD. The error bars are standard errors, from an average of 35 slices at each time point. The data have been normalized to the 30-min time point. (B) Development of injury over time after 30 min OGD. The error bars are standard errors from an average of 35 slices at each time. The data have been normalized to the 24-h time point. (C) The addition of 0.5 atm of helium had no effect on the OGD or sham-treated slices. The error bars are standard errors from an average of 34 slices at each condition. The data have been normalized to OGD with 0.5 atm helium.

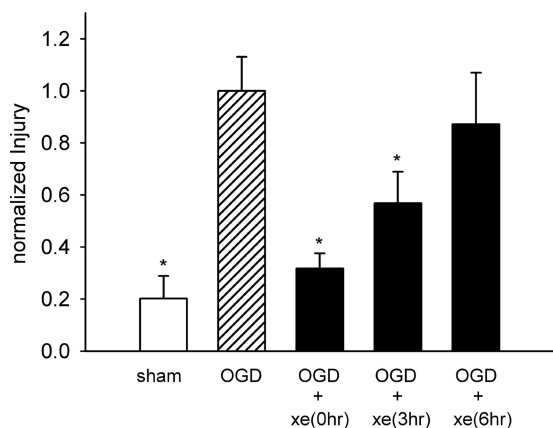


Fig. 3. Xenon (xe) provides neuroprotection when applied up to 3 h after oxygen-glucose deprivation (OGD). The bars show the protective effect of 50% atm xenon applied immediately after OGD (0 h) and 3 and 6 h after OGD. The greatest degree of protection was observed when xenon was applied immediately ($32 \pm 6\%$ of the control injury), but significant protection was observed even when xenon was applied 3 h after OGD ($57 \pm 12\%$). Sham slices were not exposed to OGD but received the same treatment and number of solution exchanges as the OGD slices. The error bars are standard errors from an average of 57 slices at each condition. The data have been normalized to the control OGD. * Significantly different ($P < 0.05$) from control OGD.

sures and any effect observed can be attributed to the effect of pressure alone. We found that helium pressure had no effect on either the sham ($P = 0.68$) or the OGD slices ($P = 0.48$), as shown in figure 2C. Although we cannot exclude the possibility that helium and pressure have equal and opposite effects on injury that exactly cancel, we believe that this result is likely to reflect a lack of effect of pressure *per se*. Nonetheless, in the xenon experiments, the OGD and sham-treated slices had 0.5 atm helium added as a control.

Having established a protocol that produced a consistent and reproducible OGD-induced injury, we next went on to investigate the effects of xenon on the development of injury. These results are shown in figure 3, where the black bars represent the effect of adding 50% atm xenon immediately after OGD or after a delay of 3 or 6 h. When xenon was applied immediately after OGD, there was robust protection against injury ($32 \pm 6\%$ of control injury), with the xenon-treated OGD slices not significantly different ($P = 0.14$) from the sham-treated slices not exposed to OGD. Even if xenon treatment was delayed until 3 h after the OGD, there was a significant ($P = 0.015$) protection, with xenon-treated slices ($57 \pm 12\%$ of the untreated control injury). However, delaying xenon treatment for 6 h resulted in no protection against OGD ($P = 0.52$). Hence, there seems to be a therapeutic time window of at least 3 h after injury in which xenon treatment is effective.

Because the aim of our study was to determine the mode of action of xenon as a neuroprotectant, we next investigated the mechanism of neuroprotection against hypoxic-ischemic injury. The drug gavestinel (4,6-dichloro-3-[(1E)-3-oxo-3-(phenylamino)-1-propenyl]-1H-indole-2-carboxylic acid) is

a prototypic NMDA receptor glycine site antagonist. We investigated whether gavestinel neuroprotection could be modulated by changing the external glycine concentration, as would be predicted if glycine site inhibition is responsible for the neuroprotective properties of gavestinel. Figure 4A shows that in the absence of added glycine, 0.5 μM gavestinel (gray bars) provided protection against OGD ($63 \pm 10\%$ of control injury) and 5 μM gavestinel (black bars) gave further protection ($36 \pm 9\%$ of control injury) compared with untreated slices. When 100 μM glycine was added to the media, there was no change to the control OGD slices (hatched bars). We chose a concentration of 100 μM glycine because this is a saturating concentration¹⁰ for the NR1/NR2A and NR1/NR2B subunit combinations that predominate in the hippocampus. In the presence of 100 μM glycine, neuroprotection by gavestinel was abolished. Treatment with 0.5 μM gavestinel (gray bars) resulted in injury ($112 \pm 13\%$ of control), and treatment with 5 μM gavestinel (black bars) resulted in injury ($67 \pm 14\%$ of control), neither of which were significantly ($P = 0.67$ and $P = 0.08$, respectively) different from the control OGD. These data confirm that gavestinel is exerting its neuroprotective effect by acting at the NMDA receptor glycine site and that we can reverse the neuroprotective action by increasing the glycine concentration. Having established that we can modulate gavestinel neuroprotection by altering the glycine concentration, we then went on to investigate whether the same was true for xenon neuroprotection. Although xenon has been shown to inhibit NMDA receptors by acting at the glycine site,¹⁰ it is not known whether this inhibition is actually involved in the neuroprotective properties of xenon. Figure 4B shows the effect of adding glycine on the neuroprotection by xenon applied immediately after OGD. In the absence of added glycine, 50% atm xenon (black bars) gave significant ($P = 0.000009$) neuroprotection, $32 \pm 6\%$ of control. Adding 100 μM glycine resulted in a small, but not significant, decrease in the control OGD injury ($83 \pm 17\%$ of OGD without glycine). However, in the presence of 100 μM glycine, xenon neuroprotection (black bars) was abolished. To rule out any possible involvement of the inhibitory glycine receptor, we performed experiments in the presence of 100 nM strychnine, a concentration that has been shown to abolish inhibitory glycine receptor activity at glycine concentrations of up to 300 μM .¹⁴ The addition of strychnine had no effect on the control OGD, xenon neuroprotection without glycine, or the reversal of xenon neuroprotection by glycine (fig. 4B). In the presence of strychnine, 50% xenon provided significant ($P = 0.0008$) neuroprotection, $38 \pm 11\%$ of the control. Adding glycine in the presence of strychnine abolished xenon neuroprotection ($P = 0.88$ compared with control OGD without xenon). Given that this rules out involvement of the inhibitory glycine receptor, the finding that xenon neuroprotection is reversed at increased glycine concentrations is consistent with xenon neuroprotection being mediated by competitive inhibition of the NMDA receptor at the glycine site.

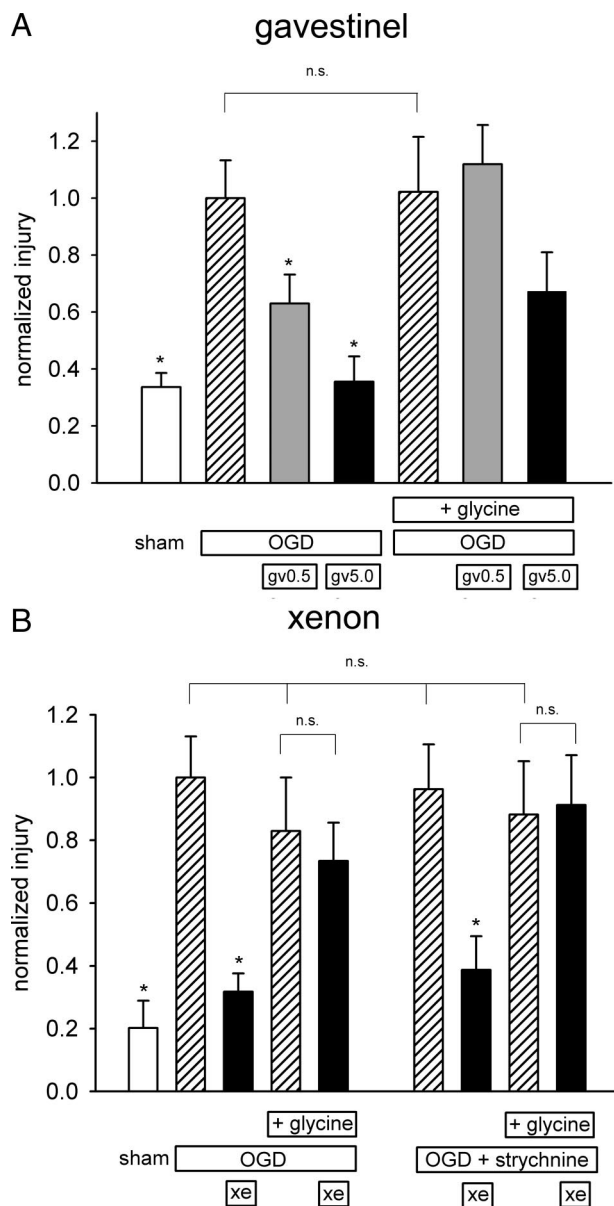


Fig. 4. (A) Gavestinel (gv) neuroprotection is reversed by adding glycine. Neuroprotection by the prototypical glycine site antagonist gavestinel is attenuated by adding glycine (100 μ M). In the absence of added glycine, gavestinel, 0.5 μ M (gray bars) and 5 μ M (black bars) reduces injury to $63 \pm 10\%$ and $36 \pm 9\%$ of control injury, respectively. Adding glycine abolishes protection by 0.5 μ M and 5 μ M gavestinel. The error bars are standard errors from an average of 48 slices at each condition. The data have been normalized to the control oxygen-glucose deprivation (OGD) with no added glycine. (B) Xenon (xe) neuroprotection is reversed by adding glycine. In the absence of added glycine, 50% atm xenon (black bars) gives robust protection ($32 \pm 6\%$ of control injury). Adding glycine (100 μ M) caused a small, but not significant, reduction in control OGD injury. However, the protective effect of 50% atm xenon was abolished. Addition of the inhibitory glycine receptor antagonist strychnine (100 nm) had no effect on control OGD (with or without glycine), xenon neuroprotection without glycine, or the reversal of xenon neuroprotection by glycine. The error bars are standard errors from an average of 44 slices at each condition. The data have been normalized to the control OGD with no added glycine. * Significantly different ($P < 0.05$) from control OGD. The four control OGD groups were compared using analysis of variance with Tukey *post hoc* test and were not significantly (n.s.) different ($P > 0.97$).

Discussion

We investigated the mechanism of neuroprotection by the anesthetic gas xenon in an *in vitro* model of hypoxia-ischemia. Cultured hippocampal mouse brain slices were subjected to OGD, and neurologic injury was quantified by PI fluorescence. Organotypic hippocampal cultures retain a heterogeneous population of cell types whose synaptic connectivity mirrors that seen *in vivo*^{15–19} and thus they represent a useful intermediate between dissociated cell cultures and whole animal models. As is the case with all models, the model we used has both advantages and limitations. We chose to use this *in vitro* model because it allows us to control the slice environment, in particular the concentration of glycine, and allows an accurate determination of duration of the insult. Although *in vivo* models preserve features lacking in the slice (such as the effect of changes in blood pressure), it would be impossible to control the glycine concentrations, as required in this study, using an *in vivo* model. Organotypic brain-slice cultures subjected to OGD have been used as a model of cerebral ischemia,^{20–24} and there is a large body of evidence that *in vitro* OGD results in changes in neuronal function that are similar to the processes occurring during ischemia *in vivo*.^{25–27}

Within a few hours of OGD, bright PI fluorescence was evident that could clearly be distinguished from the sham-treated slices (fig. 1C). PI fluorescence does not distinguish between cell death *via* necrosis or apoptosis. However, the main aim of our study was to determine the role of inhibition at the NMDA receptor glycine site in xenon neuroprotection against ischemic injury overall, whether mediated *via* apoptosis or necrosis. There is some evidence that xenon neuroprotection may involve apoptosis pathways⁴ downstream of the NMDA receptor. Whether this is true in our model merits investigation in future studies. Injury developed over time after OGD and was complete by 24 h (fig. 2B), similar to the time course reported in other studies.^{28,29} We chose to measure cell death and neuroprotection in the hippocampal slice as a whole to avoid subjective difficulties associated with precisely defining the boundaries of CA1, CA3, and dentate gyrus in a heterogeneous population of slices. Some areas of the hippocampus, such as CA1, are more sensitive to damage because of OGD,³⁰ and this is believed to reflect selective hippocampal damage such as that occurs after ischemic episodes consequent to cardiac arrest. Nevertheless, in studies that have examined region-specific neuroprotection against OGD by glutamate receptor antagonists and anesthetics, little regional differences in neuroprotection have been observed.^{20,22,31} Our results are qualitatively in line with these findings. As shown in figure 1C, the CA1 region is more sensitive to damage, but xenon neuroprotection seems similar throughout the slice. Our finding that 0.5 atm helium pressure had no effect on OGD-injured slices (fig. 2C) was unexpected because we had previously observed that this pressure of helium offered a degree of neuroprotection against a completely different injury, mechanical trauma, in

an organotypic slice model.³ The lack of helium protection we observe seems to indicate that different mechanisms of injury progression act in OGD-induced injury and mechanical trauma. Interestingly, a recent study³² using a different preparation (cultured cortical neurons) found that helium had a small, but significant, detrimental effect on OGD injury. The reason for the discrepancy with our findings may be due to the different preparations or differences in the OGD protocols used. Nevertheless, the lack of effect of helium pressure in our model simplifies the analysis. When we investigated the effects of 50% atm xenon applied after the OGD, we found that xenon applied immediately after OGD reduced the injury by almost 70% (see fig. 3). Indeed, xenon-treated slices subjected to OGD were not significantly different ($P = 0.14$) from the sham-treated slices not exposed to OGD. This degree of protection is particularly notable, given that in our model xenon is present only after the insult, unlike in some models where the neuroprotectant is also present before and during the insult. Our protocol ensures that the insult itself remains a constant and that any neuroprotection cannot be explained simply by an attenuation of the primary insult. This situation more closely models those clinical scenarios in which a patient presents for treatment after the ischemic episode.

In terms of assessing potential clinical strategies, it is important to understand the therapeutic time window in which a treatment remains effective. We therefore examined the effects of 50% atm xenon applied 3–6 h after the OGD. These results were encouraging and showed that even after a delay of 3 h xenon still retained a significant degree of neuroprotection of ~40% (see fig. 3). However, by 6 h after OGD, xenon was no longer neuroprotective (see fig. 3). This is consistent with the time course of injury in the absence of xenon (see fig. 2B), where 6 h after OGD, the injury is already well developed, reaching $64 \pm 9\%$ of its full extent, whereas at 3 h after OGD, it is only $20 \pm 4\%$ of its maximum. These findings indicate that the therapeutic window in our model extends from the time of injury until at least 3 h after injury. A similar therapeutic window for xenon neuroprotection was observed in an *in vivo* model of neonatal asphyxia,⁴ indicating the potential for xenon as a treatment after ischemia.

The main aim of this work was to determine whether xenon neuroprotection was mediated by inhibition of the NMDA receptor at its glycine-binding site. Our strategy to elucidate this was based on our observation that xenon competes with glycine and xenon inhibition of the NMDA receptor is attenuated at saturating glycine concentrations.¹⁰ We therefore sought to investigate whether the degree of neuroprotection in our *in vitro* model could be modulated by altering the glycine concentration. To validate our method, we first investigated neuroprotection by gavestinel, a known NMDA receptor glycine site antagonist. Gavestinel is a highly selective NMDA receptor glycine site antagonist³³ that has recently undergone clinical evaluation for use in stroke patients.^{34–37} We found that in the absence of added

glycine, gavestinel was neuroprotective. However, when glycine was added, gavestinel neuroprotection was abolished, with no change in the standard injury (see fig. 4A). The finding that at high glycine concentrations gavestinel neuroprotection is abolished confirms that gavestinel is acting as a neuroprotectant *via* inhibition of the NMDA receptor at the glycine site.

We next investigated whether xenon neuroprotection could similarly be modulated by adding glycine. We found that in the absence of added glycine, 50% atm xenon resulted in robust neuroprotection, reducing injury by ~70% (fig. 4B). However, adding $100 \mu\text{M}$ glycine abolished xenon neuroprotection completely. The addition of strychnine had no effect on control OGD or the reversal of xenon neuroprotection. The lack of any effect of strychnine indicates that if inhibitory glycine receptors are present in the hippocampal slices, they do not seem to play a role in OGD injury or xenon neuroprotection against OGD. These results indicate that xenon neuroprotection against hypoxia–ischemia is indeed largely mediated by inhibition of the NMDA receptor at its glycine site. This finding is important because it clearly identifies the NMDA receptor as a target mediating xenon neuroprotection against ischemic injury. Although it was our identification that xenon was an NMDA receptor antagonist^{9,38} that led to the idea of using xenon as a neuroprotectant, until now a definitive role for NMDA receptors in xenon neuroprotection has not been established. Glutamate excitotoxicity is thought to be involved in neuropathologies such as ischemia and traumatic brain injury.^{39,40} Hence, the inhibition of NMDA receptors by xenon is plausible as a mechanism of neuroprotection. Although there is a consensus that xenon inhibits NMDA receptors, whether xenon inhibits non-NMDA glutamate receptors under physiologic conditions is less clear. α -Amino-3-hydroxy-5-methyl-4-isoxazolepropionic acid receptors at glutamatergic synapses in cultured hippocampal neurons are insensitive to xenon.^{9,38} A recent report⁴¹ indicates that α -amino-3-hydroxy-5-methyl-4-isoxazolepropionic acid receptors at excitatory synapses in the amygdala are sensitive to xenon. It remains to be determined whether inhibition of α -amino-3-hydroxy-5-methyl-4-isoxazolepropionic acid receptors has a role in xenon neuroprotection in addition to that mediated by the inhibition of NMDA receptors by xenon. Furthermore, it has become clear that there are other potential targets for xenon neuroprotection that are equally as plausible as the NMDA receptor. The two pore-domain potassium channel TREK-1 is activated by xenon,⁴² and recently xenon has been shown to activate the adenosine triphosphate-sensitive potassium (K_{ATP}) channel.⁴³ That these two potassium channels may have a role in ischemic injury is suggested by the finding that genetic ablation of either TREK-1 or K_{ATP} channels increases sensitivity to ischemia and epilepsy in *in vivo* models.^{44,45} An attractive feature of TREK-1 and K_{ATP} as putative targets mediating xenon neuroprotection is that both of these channels are active at acidic pH, such as that occurs during ischemia. On the other hand, NMDA recep-

tors are inhibited by acidic pH. During periods of acidosis, this inhibition would reduce both the damaging glutamate excitotoxicity and xenon neuroprotection *via* NMDA receptors. Whether these potassium channels play a role in acute xenon neuroprotection against ischemia remains to be determined. However, the results presented here indicate that xenon neuroprotection in our model of hypoxia–ischemia can largely be accounted for by xenon inhibition of the NMDA receptor at its glycine binding site.

Neuroprotective NMDA receptor glycine site antagonists, such as gavestinel, have been shown to be well tolerated in patients and devoid of the psychotomimetic side effects common with some NMDA receptor antagonists.⁴⁶ However, the results of clinical trials with gavestinel in acute stroke were disappointing.^{36,37} The reasons for lack of efficacy of gavestinel are not clear and may be due to variables such as the delay in treatment after the ischemia or a failure of gavestinel to reach the affected area of the brain because of poor permeation of blood–brain barrier. In the case of xenon, its low blood–gas partition coefficient and rapid onset as an anesthetic⁶ indicate that it quickly penetrates to the brain. In our study, we applied xenon only after insult and we have clearly identified the therapeutic window for xenon neuroprotection (0–3 h after OGD). Hence, xenon neuroprotection could have a role in scenarios in which it could be applied close to the time of the ischemia, such as neonatal asphyxia, in surgical patients at high risk of perioperative stroke or in patients resuscitated after cardiac arrest.

The authors thank Raquel Yustos, M.Sc. (Research Technician, Biophysics Section, Imperial College London, United Kingdom), for technical support, Mark Coburn, M.D. (Anesthesiologist, Aachen University, Aachen, Germany), for advice on the organotypic cultures, Paul Brown and Steve Norris (Manager and Technician, respectively, Physics Department Workshop, Imperial College London) for building the xenon chamber, and Neal Powell (Artist, Physics Department, Imperial College London) for the artwork.

References

- Rosamond W, Flegal K, Friday G, Furie K, Go A, Greenlund K, Haase N, Ho M, Howard V, Kissela B, Kittner S, Lloyd-Jones D, McDermott M, Meigs J, Moy C, Nichol G, O'Donnell CJ, Roger V, Rumsfeld J, Sorlie P, Steinberger J, Thom T, Wasserthiel-Smoller S, Hong Y: Heart disease and stroke statistics-2007 update: A report from the American Heart Association Statistics Committee and Stroke Statistics Subcommittee. *Circulation* 2007; 115:e69–171
- Wilhelm S, Ma D, Maze M, Franks NP: Effects of xenon on *in vitro* and *in vivo* models of neuronal injury. *ANESTHESIOLOGY* 2002; 96:1485–91
- Coburn M, Maze M, Franks NP: The neuroprotective effects of xenon and helium in an *in vitro* model of traumatic brain injury. *Crit Care Med* 2008; 36:588–95
- Ma D, Hossain M, Chow A, Arshad M, Battson RM, Sanders RD, Mehmet H, Edwards AD, Franks NP, Maze M: Xenon and hypothermia combine to provide neuroprotection from neonatal asphyxia. *Ann Neurol* 2005; 58:182–93
- Homi HM, Yokoo N, Ma D, Warner DS, Franks NP, Maze M, Grocott HP: The neuroprotective effect of xenon administration during transient middle cerebral artery occlusion in mice. *ANESTHESIOLOGY* 2003; 99:876–81
- Sanders RD, Franks NP, Maze M: Xenon: No stranger to anaesthesia. *Br J Anaesth* 2003; 91:709–17
- Hemmings HC Jr, Mantz J: Xenon and the pharmacology of fear. *ANESTHESIOLOGY* 2008; 109:954–5
- Cullen SC, Gross EG: The anesthetic properties of xenon in animals and human beings, with additional observations on krypton. *Science* 1951; 113:580–2
- Franks NP, Dickinson R, de Sousa SLM, Hall AC, Lieb WR: How does xenon produce anaesthesia? *Nature* 1998; 396:324
- Dickinson R, Peterson BK, Banks P, Simillis C, Martin JC, Valenzuela CA, Maze M, Franks NP: Competitive inhibition at the glycine site of the *N*-methyl-D-aspartate receptor by the anesthetics xenon and isoflurane: Evidence from molecular modeling and electrophysiology. *ANESTHESIOLOGY* 2007; 107:756–67
- Pearlstein RD, Beirne JP, Massey GW, Warner DS: Neuroprotective effects of NMDA receptor glycine recognition site antagonism: Dependence on glycine concentration. *J Neurochem* 1998; 70:2012–9
- Stoppini L, Buchs PA, Muller D: A simple method for organotypic cultures of nervous tissue. *J Neurosci Methods* 1991; 37:173–82
- Macklis JD, Madison RD: Progressive incorporation of propidium iodide in cultured mouse neurons correlates with declining electrophysiological status: A fluorescence scale of membrane integrity. *J Neurosci Methods* 1990; 31:43–6
- Downie DL, Hall AC, Lieb WR, Franks NP: Effects of inhalational general anaesthetics on native glycine receptors in rat medullary neurones and recombinant glycine receptors in *Xenopus* oocytes. *Br J Pharmacol* 1996; 118:493–502
- Bahr BA: Long-term hippocampal slices: A model system for investigating synaptic mechanisms and pathologic processes. *J Neurosci Res* 1995; 42:294–305
- Noraberg J, Poulsen FR, Blaabjerg M, Kristensen BW, Bonde C, Montero M, Meyer M, Gramsbergen JB, Zimmer J: Organotypic hippocampal slice cultures for studies of brain damage, neuroprotection and neurorepair. *Curr Drug Targets CNS Neurol Disord* 2005; 4:435–52
- Finley M, Fairman D, Liu D, Li P, Wood A, Cho S: Functional validation of adult hippocampal organotypic cultures as an *in vitro* model of brain injury. *Brain Res* 2004; 1001:125–32
- Crain SM: Development of specific synaptic network functions in organotypic central nervous system (CNS) cultures: Implications for transplantation of CNS neural cells *in vivo*. *Methods* 1998; 16:228–38
- Frantseva MV, Kokarovtseva L, Perez Velazquez JL: Ischemia-induced brain damage depends on specific gap-junctional coupling. *J Cereb Blood Flow Metab* 2002; 22:453–62
- Sullivan BL, Leu D, Taylor DM, Fahlman CS, Bickler PE: Isoflurane prevents delayed cell death in an organotypic slice culture model of cerebral ischemia. *ANESTHESIOLOGY* 2002; 96:189–95
- Elsersy H, Mixco J, Sheng H, Pearlstein RD, Warner DS: Selective gamma-aminobutyric acid type A receptor antagonism reverses isoflurane ischemic neuroprotection. *ANESTHESIOLOGY* 2006; 105:81–90
- Montero M, Nielsen M, Ronn LC, Moller A, Noraberg J, Zimmer J: Neuroprotective effects of the AMPA antagonist PNQX in oxygen-glucose deprivation in mouse hippocampal slice cultures and global cerebral ischemia in gerbils. *Brain Res* 2007; 1177:124–35
- Bickler PE, Warner DS, Stratmann G, Schuyler JA: γ -Aminobutyric acid-A receptors contribute to isoflurane neuroprotection in organotypic hippocampal cultures. *Anesth Analg* 2003; 97:564–71
- Laake JH, Haug FM, Wieloch T, Ottersen OP: A simple *in vitro* model of ischemia based on hippocampal slice cultures and propidium iodide fluorescence. *Brain Res Protoc* 1999; 4:173–84
- Rothman S: Synaptic release of excitatory amino acid neurotransmitter mediates anoxic neuronal death. *J Neurosci* 1984; 4:1884–91
- Goldberg MP, Choi DW: Combined oxygen and glucose

- deprivation in cortical cell culture: Calcium-dependent and calcium-independent mechanisms of neuronal injury. *J Neurosci* 1993; 13:3510-24
27. Goldberg WJ, Kadingo RM, Barrett JN: Effects of ischemia-like conditions on cultured neurons: Protection by low Na⁺, low Ca²⁺ solutions. *J Neurosci* 1986; 6:3144-51
 28. Frantseva MV, Carlen PL, El-Beheiry H: A submersion method to induce hypoxic damage in organotypic hippocampal cultures. *J Neurosci Methods* 1999; 89:25-31
 29. Bonde C, Norberg J, Zimmer J: Nuclear shrinkage and other markers of neuronal cell death after oxygen-glucose deprivation in rat hippocampal slice cultures. *Neurosci Lett* 2002; 327:49-52
 30. Rytter A, Cronberg T, Asztely F, Nemali S, Wieloch T: Mouse hippocampal organotypic tissue cultures exposed to *in vitro* "ischemia" show selective and delayed CA1 damage that is aggravated by glucose. *J Cereb Blood Flow Metab* 2003; 23:23-33
 31. Gray JJ, Bickler PE, Fahlman CS, Zhan X, Schuyler JA: Isoflurane neuroprotection in hypoxic hippocampal slice cultures involves increases in intracellular Ca²⁺ and mitogen-activated protein kinases. *ANESTHESIOLOGY* 2005; 102:606-15
 32. Jawad N, Rizvi M, Gu J, Adeyi O, Tao G, Maze M, Ma D: Neuroprotection (and lack of neuroprotection) afforded by a series of noble gases in an *in vitro* model of neuronal injury. *Neurosci Lett* 2009; 460:232-6
 33. Di Fabio R, Capelli AM, Conti N, Cugola A, Donati D, Feriani A, Gastaldi P, Gaviraghi G, Hewkin CT, Micheli F, Missio A, Mugnaini M, Pecunioso A, Quaglia AM, Ratti E, Rossi L, Tedesco G, Trist DG, Reggiani A: Substituted indole-2-carboxylates as *in vivo* potent antagonists acting as the strychnine-insensitive glycine binding site. *J Med Chem* 1997; 40:841-50
 34. Haley EC Jr, Thompson JL, Levin B, Davis S, Lees KR, Pittman JG, DeRosa JT, Ordroneau P, Brown DL, Sacco RL: Gavestinel does not improve outcome after acute intracerebral hemorrhage: An analysis from the GAIN International and GAIN Americas studies. *Stroke* 2005; 36:1006-10
 35. Warach S, Kaufman D, Chiu D, Devlin T, Luby M, Rashid A, Clayton L, Kaste M, Lees KR, Sacco R, Fisher M: Effect of the glycine antagonist gavestinel on cerebral infarcts in acute stroke patients, a randomized placebo-controlled trial: The GAIN MRI Substudy. *Cerebrovasc Dis* 2006; 21:106-11
 36. Sacco RL, DeRosa JT, Haley EC Jr, Levin B, Ordroneau P, Phillips SJ, Rundek T, Snipes RG, Thompson JL: Glycine antagonist in neuroprotection for patients with acute stroke: GAIN Americas: A randomized controlled trial. *JAMA* 2001; 285:1719-28
 37. Lees KR, Asplund K, Carolei A, Davis SM, Diener HC, Kaste M, Orgogozo JM, Whitehead J: Glycine antagonist (gavestinel) in neuroprotection (GAIN International) in patients with acute stroke: A randomised controlled trial. *GAIN International Investigators. Lancet* 2000; 355:1949-54
 38. de Sousa SLM, Dickinson R, Lieb WR, Franks NP: Contrasting synaptic actions of the inhalational general anesthetics isoflurane and xenon. *ANESTHESIOLOGY* 2000; 92:1055-66
 39. Bullock R, Zauner A, Myseros JS, Marmarou A, Woodward JJ, Young HF: Evidence for prolonged release of excitatory amino acids in severe human head trauma: Relationship to clinical events. *Ann N Y Acad Sci* 1995; 765:290-7
 40. Nilsson P, Hillered L, Ponten U, Ungerstedt U: Changes in cortical extracellular levels of energy-related metabolites and amino acids following concussive brain injury in rats. *J Cereb Blood Flow Metab* 1990; 10:631-7
 41. Haseneder R, Kratzer S, Kochs E, Eckle VS, Zieglgansberger W, Rammes G: Xenon reduces *N*-methyl-D-aspartate and alpha-amino-3-hydroxy-5-methyl-4-isoxazolepropionic acid receptor-mediated synaptic transmission in the amygdala. *ANESTHESIOLOGY* 2008; 109:998-1006
 42. Gruss M, Bushell TJ, Bright DP, Lieb WR, Mathie A, Franks NP: Two-pore-domain K⁺ channels are a novel target for the anesthetic gases xenon, nitrous oxide, and cyclopropane. *Mol Pharmacol* 2004; 65:443-52
 43. Bantel C, Maze M, Trapp S: Neuronal preconditioning by inhalational anesthetics: Evidence for the role of plasmalemmal adenosine triphosphate-sensitive potassium channels. *ANESTHESIOLOGY* 2009; 110:986-95
 44. Heurteaux C, Guy N, Laigle C, Blondeau N, Duprat F, Mazzuca M, Lang-Lazdunski L, Widmann C, Zanzouri M, Romey G, Lazdunski M: TREK-1, a K⁺ channel involved in neuroprotection and general anesthesia. *EMBO J* 2004; 23:2684-95
 45. Yamada K, Ji JJ, Yuan H, Miki T, Sato S, Horimoto N, Shimizu T, Seino S, Inagaki N: Protective role of ATP-sensitive potassium channels in hypoxia-induced generalized seizure. *Science* 2001; 292:1543-6
 46. Dyker AG, Lees KR: Safety and tolerability of GV150526 (a glycine site antagonist at the *N*-methyl-D-aspartate receptor) in patients with acute stroke. *Stroke* 1999; 30:986-92